Rechargeable lithium cells with dendrite-free electrodeposited lithium on aluminium as negative electrode

P. Suresh [a], A.K. Shukla [a], S.A. Shivashankar [b], N. Munichandraiah [c,*]

[a] *Solid State and Structural Chemistry Unit, Indian Institute of Science, Bangalore-560 012, India*
[b] *Materials Research Center, Indian Institute of Science, Bangalore-560 012, India*
[c] *Department of Inorganic and Physical Chemistry, Indian Institute of Science, Bangalore-560 012, India*

Abstract

The dendrite-free cathodic deposition of lithium on an aluminium substrate and its anodic stripping are found to occur reversibly within ± 0.1 V versus Li/Li$^+$ in an aprotic electrolyte. It is possible to envisage a novel route to realise rechargeable Li (Al)–LiCoO$_2$ and Li (Al)–LiMn$_2$O$_4$ cells. Several rechargeable Li (Al)–LiCoO$_2$ and Li (Al)–LiMn$_2$O$_4$ cells of varying capacities up to 65 mAh have been assembled in-house, and evaluated at different charge–discharge rates as well as at various temperatures. Consistent capacity values are obtained with these rechargeable cells over about 50 cycles.
© 2004 Elsevier B.V. All rights reserved.

1. Introduction

Non-aqueous batteries with lightweight lithium metal are desirable for electric vehicles due to their high energy and power densities in relation to the present-day lithium-ion cells. Several studies have been reported [1,2] on rechargeable non-aqueous batteries with lithium as the negative electrode. Although primary cells have been realised commercially, secondary cells employing Li-metal are beset with problems such as surface passivation, dendritic growth of Li, internal shorting, build-up of cell pressure during repeated cycling, electrical isolation of active Li, increase in internal resistance, thermal instability, cell explosion, etc. [3,4]. Consequently, research and development efforts have been expended to investigate alternate anode materials, such as carbon, which could act as a host for insertion and extraction of Li$^+$-ions reversibly. In recent years, the commercialisation of Li-ion cells employing carbon-based insertion electrodes has constituted a break-through in the area of rechargeable batteries [5]. The capacity value of carbon-based anodes, namely C$_6$Li, in Li-ion cells is only about 380 mAh g^{-1} against a capacity value of about 3800 mAh g^{-1} for Li metal [6]. The capacity of the C$_6$Li is therefore only 10% of the capacity expected for metallic Li.

Accordingly, a Li metal-based negative electrode, free from the aforesaid problems, would provide enhanced capacity and facilitate the development of rechargeable Li cells with specific energy values that would be substantially higher than Li-ion cells.

Recently, we have studied the electrochemical stability of Al in an aprotic electrolyte, generally used in Li-ion cells, over a wide potential range [7]. It was observed that while Al is stable up to 3.5 V versus Li/Li$^+$ in the positive potential (anode) direction, its electrochemical stability decreases at potentials beyond 3.5 V versus Li/Li$^+$ due to the anodic breakdown of the surface passivating film. In the negative potential (cathode) direction, a smooth, uniform and non-dendritic electrodeposition of Li occurs on Al. Both the cathodic deposition of Li and its anodic stripping have been found to be reversible in the potential range close to the reversible potential of Li/Li$^+$ couple [7], which suggests that a Li deposited Al electrode (hereafter referred to as a Li (Al) electrode) could be used as the negative electrode for rechargeable Li cells.

In the present study, Li (Al)–LiCoO$_2$ and Li (Al)–LiMn$_2$O$_4$ cells of varying capacities have been assembled, and characterised electrochemically. The cells have been subjected to several charge–discharge cycles without any noticeable decline in their capacities. The study signifies the application of Al as the negative electrode substrate for high-energy rechargeable Li batteries.

---

* Corresponding author. Tel.: +91-80-2933-183; fax: +91-80-3600-683.
E-mail address: muni@ipc.iisc.ernet.in (N. Munichandraiah).

2. Experimental

Ethylene carbonate (EC), dimethyl carbonate (DMC), $LiBF_4$, $LiCoO_2$, $LiMn_2O_4$, and Li (0.75 mm thick) metal were purchased from Aldrich. The solvents (EC and DMC) were distilled, mixed in equal volumes, and percolated through molecular sieves of grade 4 Å. The solid compounds were dried at 100 °C prior to their use.

Aluminium sheet of 0.2 mm thick was used for the negative electrode as well as for the substrate of the positive electrode. It was polished, using successive grades of emery, to a smooth surface, then washed with a detergent, rinsed with distilled water, dipped in acetone, air-dried and stored in a vacuum desiccator. For the purpose of making the positive electrode, 65 wt.% $LiCoO_2$ (or $LiMn_2O_4$), 25 wt.% acetylene black and 10 wt.% polyvinylidene fluoride were mixed using n-methyl-pyrrolidinone to form a homogeneous paste, which was spread on to a pre-treated Al foil followed by drying at 80 °C under vacuum. The spreading of the mix and drying steps were repeated three times and the electrodes thus obtained were finally dried at 80 °C under vacuum for about 12 h. The electrolyte was a 1 M solution of $LiBF_4$ dissolved in the mixed solvents.

Small cells were assembled in airtight glass containers, whereas rectangular polypropylene containers were used for the assembly of larger cells. For cells of 10 mAh and higher capacities, the size of the electrodes was 3 cm × 2 cm with a geometrical area of 12 cm^2. The electrodes were stacked together by sandwiching the positive and negative electrodes using a microporous polypropylene (Celgard 2400) separator. A Li strip was introduced into each cell and was used as the reference electrode. The electrolyte was added and the container was closed using an airtight lid.

Preparation of the electrolyte and assembly of the cells were conducted in an argon atmosphere (MBraun Dry Box Model Unilab) with both the moisture and oxygen levels less than 10 ppm. Galvanostatic charge–discharge cycling was performed using a circuit that comprised a regulated dc power supply, a high resistance, and an ammeter in series with the cell. For performing experiments in the temperature range between 0 and 40 °C, a refrigerator-cum-heater (Julabo Model-F25) was employed. At each temperature, the cells were equilibrated for 3 h prior to the measurements. All the measurements were repeated and found to be reproducible. The X-ray diffraction (XRD) pattern of the Li (Al) specimen was recorded using a powder X-ray diffractometer (Scintag Model XDS 2000) and the surface morphology was examined by a scanning electron microscope (SEM, Jeol Model JSM 5600LV).

3. Results and discussion

Electrodeposition of Li from the non-aqueous electrolyte was studied on Al as well as Li substrates for the sake of comparison. Galvanostatic charging (cathodic deposition)

and discharging (anodic stripping) were carried out repeatedly at a current density of 10 mA cm^{-2}, and the potentials of Li and Al were monitored while observing the nature of the surface on the substrate. An in situ physical examination under an optical microscope revealed that the deposition of Li on a Li substrate is dendritic within the first few cycles, subsequently changes to a porous bulky mass, and some of it becomes detached from the substrate while some of it grows towards the auxiliary electrode which is kept several mm apart. By contrast, the deposition of Li on Al substrate is found to be uniform, non-dendritic and adherent to the substrate over a large number of cycles. The potential values measured during the charging and discharging processes indicate that the potential of the Al substrate is within ±0.1 V versus Li/Li$^+$ as compared with a value near 0 V versus Li/Li$^+$ for the Li substrate.

A Li (Al) electrode, which was subjected to several cycles, was separated from the electrochemical cell in a discharged condition and examined by XRD and SEM [7]. The electrode surface was grey in colour even after anodic striping of Li, and subsequent washing with water. It was expected that the metallic Li present on the surface, if any, could be removed by oxidation with water. Persistent appearance of grey colour thus suggested that it is not due to metallic Li on the Al surface, but due to Li, which has penetrated into Al and caused the formation of Al–Li alloy. This was confirmed by comparing the XRD patterns of unused Al and grey Al formation (Fig. 1). The XRD pattern of Al specimen matches with the standard pattern of Al (Fig. 1(a)). There are, however, additional peaks at 2θ values of 24.2, 40.1, 47.5, 58.1,
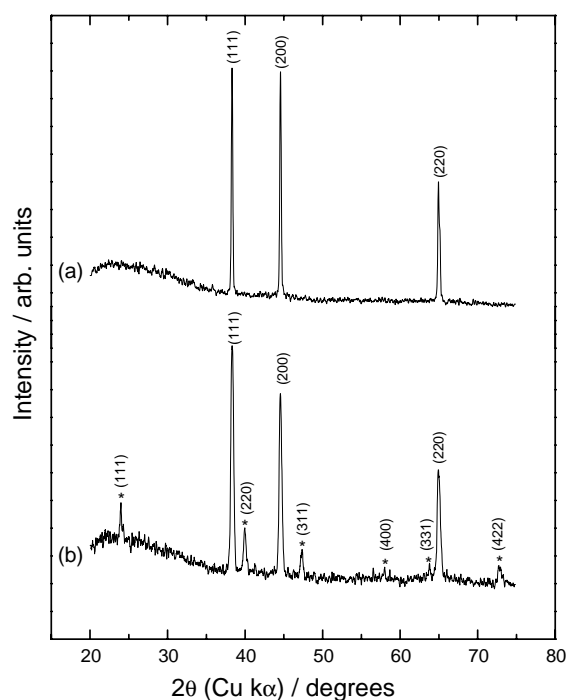

Fig. 1. XRD patterns of (a) Al and (b) Li–Al alloy. Reflections marked (*) correspond to Al–Li alloy.
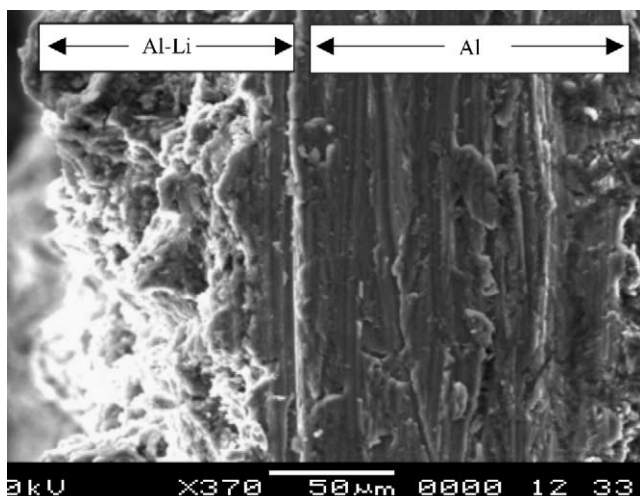
Fig. 2. Electron micrograph of cross-section of Li (Al) electrode after 50 cycles.

63.8 and 79.9° (Fig. 1(b)), which correspond to the Al–Li composition [8]. The surface of the Al specimen was examined with a scanning electron microscope [7]. Micro cracks were present which were distributed uniformly over the entire surface due to stresses that are caused on insertion of Li into Al that results in the formation of the Al–Li alloy. Furthermore, an examination of SEM micrographs (Fig. 2) over a cross-section of the grey Al specimen suggests that only a surface layer of about 100 μm in thickness is alloyed with Li. It is thus inferred that the Al–Li formation is limited to the outer layers of the Al electrode and does not progress to the bulk Al during prolonged cycling. It has been known that Li and Al form two [9] or three [10] alloys. The Li-rich phase is known as the α-phase and the Al-rich phase with a nominal composition of Li–Al is known as the β-phase. The XRD pattern shown in Fig. 1(b) corresponds to the composition of the Al–Li alloy [8], which suggests that insertion of excess Li into Al does not occur under the present experimental conditions. It is noteworthy that Li–Al alloys have been extensively studied [11,12] as possible anodes to replace Li. These approaches have not been successful, however, most probably due to the low diffusivity of Li in Li–Al alloys.

The morphology of an electrodeposited layer generally depends on the nature of the substrate. It is known that both Li and Al substrates are covered with surface passive films, irrespective of the pre-treatment procedure adopted before using them for the experiments [13,14]. The passivating layers on these two metals possess different properties relative to their composition, thickness, porosity, density, conductivity, etc. It is inferred from the present study that the Al surface is more conducive to nondendritic deposition of Li than the Li substrate.

The Li (Al)–LiCoO$_2$ and Li (Al)–LiMn$_2$O$_4$ cells were present in their discharged state and their open-circuit voltages were between 0.3 and 0.5 V on assembling them with Al as the negativ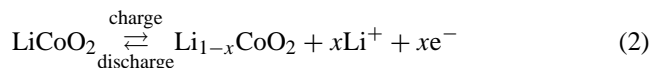e electrode. The cells were subsequently subjected to galvanostatic charging, and the electrode potentials along with the cell voltage were monitored. Typical charge and discharge data exhibiting the variation of electrode potential and cell voltage for a Li (Al)–LiCoO$_2$ cell of about 30 mAh capacity are shown in Fig. 3(a) and (b), respectively; similar data for a Li (Al)–LiMn$_2$O$_4$ cell of capacity about 25 mAh are shown in Fig. 3(c) and (d), respectively.

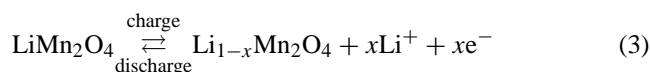The electrode reactions for the cells are as follows.

At the Al negative electrode:

$$Al + Li^+ + e^- \underset{discharge}{\overset{charge}{\rightleftarrows}} Li(Al) \tag{1}$$
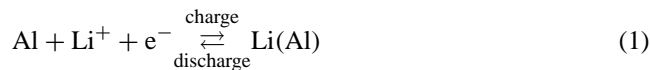
At the LiCoO$_2$ positive electrode:

$$LiCoO_2 \underset{discharge}{\overset{charge}{\rightleftarrows}} Li_{1-x}CoO_2 + xLi^+ + xe^- \tag{2}$$

At the positive electrode of the Li (Al)–LiMn$_2$O$_4$ cell:

$$LiMn_2O_4 \underset{discharge}{\overset{charge}{\rightleftarrows}} Li_{1-x}Mn_2O_4 + xLi^+ + xe^- \tag{3}$$

The charging of the cells was continued until the potential of the positive electrode attained 4.2 V versus Li/Li$^+$. By charging up to this value of potential, it is known [15] that nearly 50% of Li initially present in the LiCoO$_2$ is extracted, i.e., $x \approx 0.5$ in reaction (2). The potential of the Al electrode was within ±0.1 V versus Li/Li$^+$ soon after commencing the charging process, which indicates the deposition of Li on Al according to the forward process for reaction (1). After termination of charging, the cells attained a stable open-circuit voltage close to 3.75 V. During the discharge of the cells, the reverse processes for reactions (1)–(3) occur. The discharge was continued until the potential of the negative electrodes reached a value of about 1.5 V versus Li/Li$^+$. The voltage drop at the beginning of the discharge of the cell provided an internal resistance of less than 0.8 Ω for the cells. At the C/5 rate of charge–discharge cycling, the nominal capacity value of the Li (Al)–LiCoO$_2$ cell was 30 mAh while it was 25 mAh for Li (Al)–LiMn$_2$O$_4$ cell. Li (Al)–LiCoO$_2$ and Li (Al)–LiMn$_2$O$_4$ cells of several capacity values up to 60 mAh were assembled and cycled for about 50 cycles. In all these cells, discharge capacities of about 110 mAh g^{-1} for both LiCoO$_2$ and LiMn$_2$O$_4$ were obtained, which compare well with the literature values reported for LiCoO$_2$ (~140 mAh g^{-1}) and LiMn$_2$O$_4$ (~110–120 mAh g^{-1}) [16–23].

The cells were evaluated for their discharge capacities at several discharge rates between C and C/5. The corresponding discharge curves for Li (Al)–LiCoO$_2$ and Li (Al)–LiMn$_2$O$_4$ cells are shown in Fig. 4(a) and (b), respectively. At all discharge rates, the major component of the discharge capacity is achieved in the voltage range between 4 and 3 V. The discharge capacity obtained at the C/5 rate is taken as the nominal capacity of the cells. Typically for the Li (Al)–LiCoO$_2$ cell, there is a decrease of about 17% in capacity on increasing the discharge rate from C/5 to C.
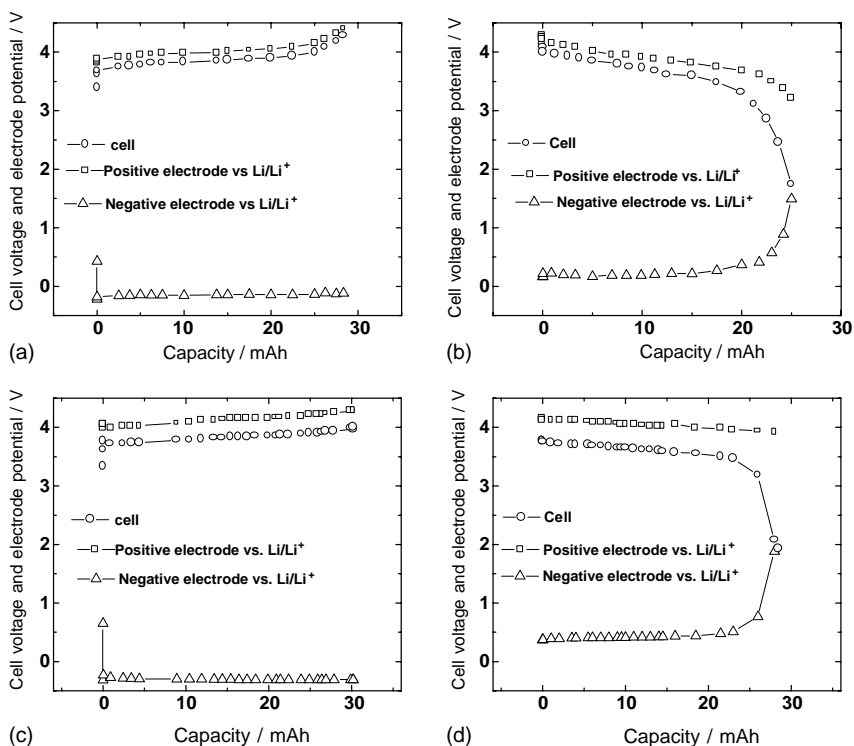
Fig. 3. (a) Typical cell charge data for 30 mAh capacity Li (Al)–LiCoO$_2$ cell and (b) its discharge data. (c) Typical cell charge data for 25 mAh capacity Li (Al)–LiMn$_2$O$_4$ cell and (d) its discharge data at C/5 rate at 25 °C.
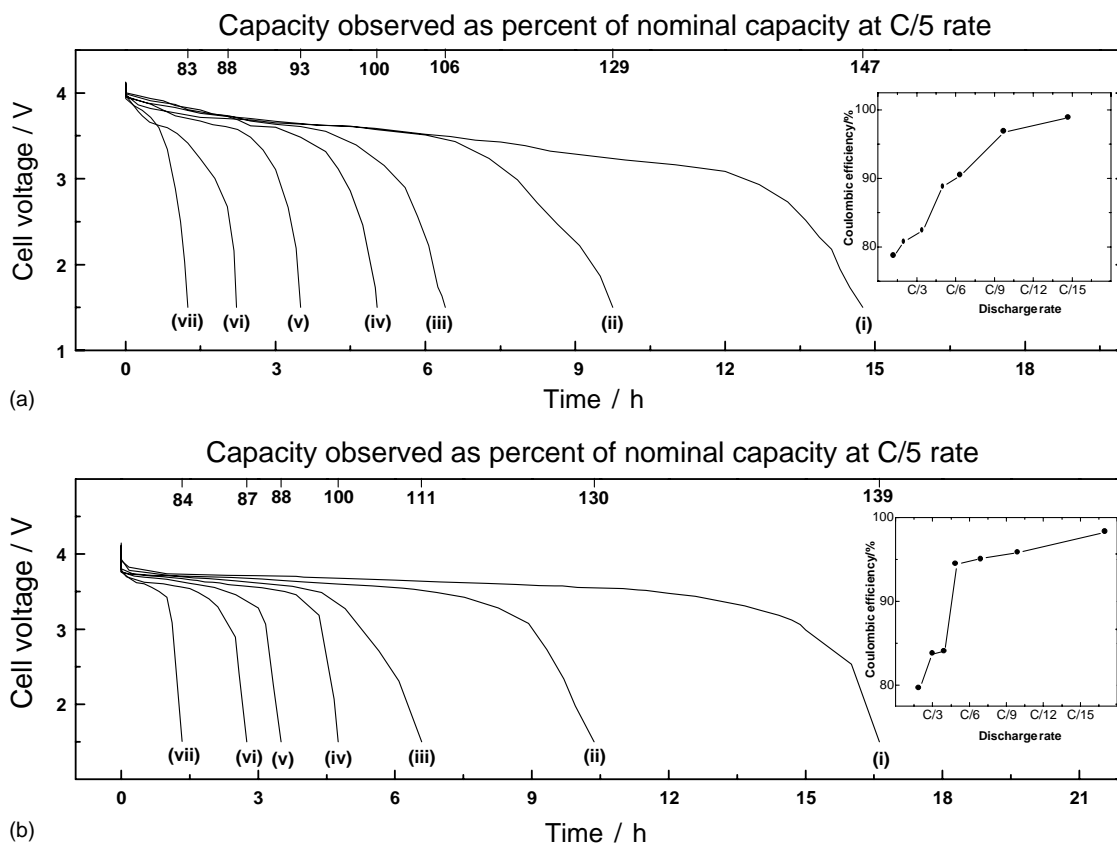

Fig. 4. Typical discharge curves at 25 °C (a) for Li (Al)–LiCoO$_2$ cell and (b) for Li (Al)–LiMn$_2$O$_4$ cell at: (i) C/17; (ii) C/11; (iii) C/7; (iv) C/5; (v) C/4; (vi) C/3; and (vii) C rates. Variations of coulombic efficiency with cycling rate are shown in the inset.

On the other hand, there is an increase of about 47% in capacity on decreasing the discharge rate from $C/5$ to $C/15$. At low discharge rates, the coulombic efficiency of the cells is nearly 100%, but there is a decrease in coulombic efficiency with an increase in the discharge rate (inset Fig. 4(a) and (b)). For instance, the coulombic efficiency values are about 98.8% at the $C/15$ rate and about 78.6% at the C rate for the Li (Al)–LiCoO$_2$ cell. The decrease in capacity (Fig. 4) and in coulombic efficiency with increasing discharge rate is most likely due to the decreased utilisation efficiency of the negative electrode.

Both Li (Al)–LiCoO$_2$ and Li (Al)–LiMn$_2$O$_4$ cells were subjected to cycling at different temperatures between 0 and 40 °C. The discharge capacity data for the cells versus temperature are shown in Fig. 5. There is a decrease in capacity with decreasing temperature similar to the variation of capacity of Li-ion cells [24]. For instance, there is a decrease in capacity of the Li (Al)– LiCoO$_2$ cell from 30 mAh at ambient temperature to about 15 mAh at 0 °C. On the other hand, there is an increase in capacity to about 45 mAh at 40 °C. The low capacity values are attributed to poor kinetics for electrode reactions at sub-ambient temperatures. The cells were subjected to an extended cycle-life test, and the data for three different cells are shown in Fig. 6. The discharge capacities are fairly stable over 50 cycles carried out for both types of cells.

Some of the discharged cells were opened after 50 cycles and the Li (Al) electrodes were examined by both XRD and SEM. The XRD pattern is similar to the data shown in Fig. 1, which confirms the formation of Al–Li alloy [8]. The alloy formation was limited to the outer surface layer and did not extend to the bulk of the Al electrode, even after 50 cycles. The mechanical stability of the Li (Al) negative electrode is thus ensured.
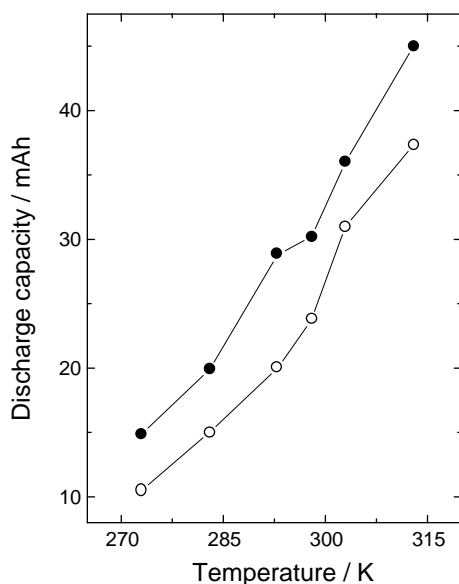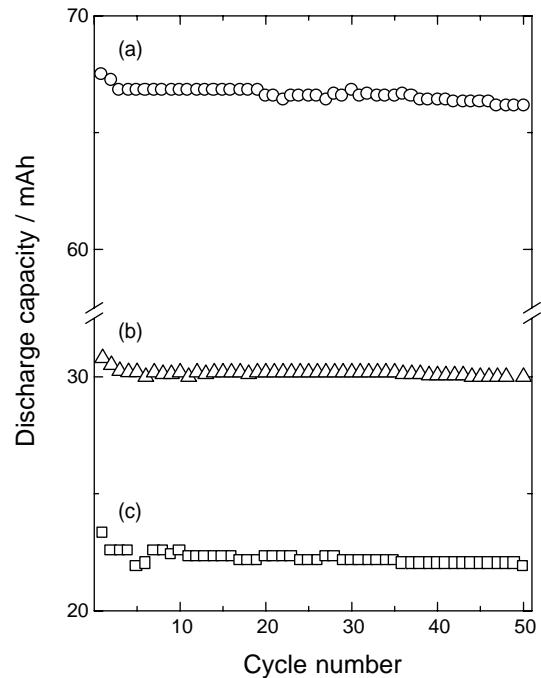

Fig. 6. Variation in discharge capacity values of (a) 30 mAh capacity Li (Al)–LiCoO$_2$ cell; (b) 25 mAh capacity Li (Al)–LiMn$_2$O$_4$ cell; and (c) 65 mAh capacity Li (Al)–LiMn$_2$O$_4$ cell over 50 cycles tested at ambient temperature.

It is noteworthy that akin to the present study, cells employing Ni as the substrate for Li negative electrode have been assembled and evaluated [25]. Nickel is, however, both expensive and heavier than Al. From the above results, it is evident that Al could be an attractive substrate for the negative electrodes in rechargeable Li batteries. Although several other aspects, such as a longer tests of cycle-life than that reported in this study need to be investigated, it is anticipated that the dendrite-free growth of the Li deposit during cycling would ameliorate the performance of the cells. Furthermore, by using Al instead of Li as the substrate, the quantity of the reactive Li would be reduced substantially. In the discharged state, metallic Li is virtually absent in the cell. Thus, it is likely that Li (Al)-based rechargeable cells would also be safer. A copper substrate is presently used for making carbon-based negative electrodes in Li-ion batteries. By employing a lighter Al substrate, there would be a definite reduction in the mass of the substrate. As a consequence, the mass of the negative electrode would be reduced, and also its fabrication would be both easier as well as cheaper.

These aspects, combined with the higher capacity of Li in relation to carbon, would help to enhance the specific energy of rechargeable Li (Al) batteries from the present 120–140 Wh kg^{-1} value for Li-ion batteries [26].

4. Conclusions

Dendrite-free cathodic deposition of Li on a Al substrate results in a novel Li (Al) negative electrode which could

Fig. 5. Discharge capacity vs. temperature of cycling of (●) Li (Al)–LiCoO$_2$ cell and (○) Li (Al)–LiMn$_2$O$_4$ cell.

be employed for fabricating rechargeable Li (Al)–LiCoO$_2$ and Li (Al)–LiMn$_2$O$_4$ cells. Lithium rechargeable cells of up to about 65 mAh have been assembled and tested over 50 cycles with consistent capacity outputs. This indicates the possibility of employing Al as substrate for negative electrodes in high-energy lithium rechargeable cells.

Acknowledgements

References

[1] S.B. Brummer, in: E.B. Yeager, B. Schumm, G. Blomgren, D.R. Blankenship, V. Leger, J. Akridge (Eds.), Lithium Non-aqueous Battery Electrochemistry, The Electrochemical Society Proceedings Series, Princeton, NJ, USA, 1980, Proc. vol. 80–7, pp. 130–142.

[2] E. Peled, J. Power Sources 6 (1981) 357.

[3] J.P. Gabano, in: J.P. Gabano (Ed.), Lithium Batteries, Academic Press, London, UK, 1983.

[4] D. Linden, T.B. Reddy (Eds.), Handbook of Batteries, third ed., McGraw-Hill, 2002.

[5] C.A. Vincent, B. Scrosati, Modern Batteries, second ed., Arnold, London, 1997.

[6] J.R. Dahn, A.K. Sleigh, H. Shi, B.M. Way, W.J. Weydanz, J.N. Reimers, Q. Gong, U. von Sacken, in: G. Pistoia (Ed.), Lithium Batteries—New Materials, Developments and Perspectives, Elsevier, Amsterdam, 1994.

[7] P. Suresh, A.K. Shukla, S.A. Shivashankar, N. Munichandraiah, J. Power Sources 110 (2002) 11.

[8] JCPDS No: 03-1215.

[9] C.J. Wen, B.A. Boukamp, R.A. Huggins, W. Weppener, J. Electrochem. Soc. 126 (1979) 2258.

[10] A.J. McAlister, Bull. Alloy Phase Diagrams 3 (1982) 177.

[11] B.M.L. Rao, R.W. Francis, H.A. Christopher, J. Electrochem. Soc. 124 (1977) 1490.

[12] H.J. Bang, S. Kim, J. Prakash, J. Power Sources 92 (2001) 45.

[13] K. Kanamura, S. Shiraishi, Z. Takehara, J. Electrochem. Soc. 141 (1994) L108.

[14] Y. Hamon, T. Brousse, F. Jousse, P. Topart, P. Buvat, D.M. Schleich, J. Power Sources 97 (2001) 185.

[15] R. Koksbang, J. Barker, H. Shi, M.Y. Saidi, Solid State Ionics 84 (1996) 1.

[16] M.M. Thackeray, P.G. David, P.G. Bruce, J.B. Goodenough, Mater. Res. Bull. 18 (1983) 461.

[17] D. Guyomard, J.M. Tarascon, J. Electrochem. Soc. 139 (1992) 937.

[18] S.H. Park, K.S. Park, Y.-K. Sun, K.S. Nahm, J. Electrochem. Soc. 147 (2000) 2116.

[19] A.D. Pasquier, A. Blyr, P. Courjal, D. Larcher, G. Amatucci, B. Gernad, J.-M. Tarascon, J. Electrochem. Soc. 146 (1999) 428.

[20] X. Xia, Y. Zhou, M. Yoshio, J. Electrochem. Soc. 144 (1997) 2593.

[21] C. Sigala, D. Guyomard, A. Verbaere, Y. Piffard, M. Tournoux, Solid State Ionics 81 (1995) 167.

[22] H. Kawai, M. Nagata, H. Kageyama, H. Tsukamoto, A.R. West, Electrochim. Acta 45 (1999) 315.

[23] S.S. Zhang, K. Xu, T.R. Jow, Electrochem. Solid-State Lett. 5 (2002) A92.

[24] P. Suresh, A.K. Shukla, N. Munichandraiah, J. Appl. Electrochem. 32 (2002) 267.

[25] I. Stassen, G. Hambitzer, J. Power Sources 105 (2002) 145.

[26] D.A.J. Rand, R.M. Dell, Understanding Batteries, Royal Society of Chemistry, Cambridge, UK, 2001.